Optical and Quantum Electronics (2019) 51:382
https://doi.org/10.1007/s11082-019-2106-3

What limits the efficiency of GaN-based superluminescent light-emitting diodes (SLEDs)?

Joachim Piprek[1]

Received: 13 July 2019 / Accepted: 6 November 2019

Abstract
Gallium-nitride-based SLEDs are attractive light sources for augmented reality displays and other applications. However, the electrical-to-optical power conversion efficiency (PCE) of SLEDs is still far below the record-high values reported for LEDs. Utilizing advanced numerical device simulation, this paper investigates the internal physical processes that cause the low PCE of SLEDs. The poor hole conductivity strongly reduces the electrical efficiency, similar to laser diodes. However, in contrast to laser diodes, the rising carrier density in the active layers is identified as main reason for enhanced Auger recombination that severely limits the internal quantum efficiency. Design improvement options are demonstrated.

Keywords Superluminescent light-emitting diode · SLED · Laser diode · InGaN/GaN · Power conversion efficiency · Auger recombination · Hole conductivity · Self-heating

1 Introduction

GaN-based light emitters have received tremendous attention in recent years due to various applications in lighting, displays, communication and other fields. A high electrical-to-optical power conversion efficiency (PCE) is often a key requirement for these applications. GaN-based light emitting diodes (LEDs) transform up to 83% of the electrical input power into light output power (Hurni et al. 2015). GaN-based lasers reach about half that efficiency (Strauss et al. 2017), which is mainly limited by the low hole conductivity of the thick p-doped cladding layer required for wave guiding (Piprek 2017a).

Superluminescent light-emitting diodes (SLEDs) are similar to laser diodes (LDs) but are operated below lasing threshold by minimizing the optical feedback from one or both facets of the internal waveguide (Matuschek et al. 2017). SLEDs thereby produce a narrow beam of light by amplified spontaneous emission (ASE) that exhibits a relatively broad wavelength spectrum. The combination of focused and incoherent light emission results in low speckle noise which makes GaN-based SLEDs attractive light sources for compact

✉ Joachim Piprek
piprek@nusod.org

[1] NUSOD Institute LLC, Newark, DE 19714-7204, USA

projection systems (Rosetti et al. 2012). However, reported SLED power conversion efficiencies hardly exceed 10% (Castiglia et al. 2018).

Based on advanced numerical device simulation, this paper studies the physical mechanisms that cause such severe PCE limitations in GaN-based SLEDs. For comparison, we employ the same model and parameters as in our recent simulation of 405 nm InGaN/GaN LDs which produced excellent agreement with measurements (Piprek 2017a). This high-power LD featured a reflectivity of 0.95 at the back facet and 0.056 at the front facet. We here reduce the simulated front facet reflectivity to zero and thereby transform this laser into an SLED. Such reflective SLEDs with a single high-reflection facet are commonly used to increase the output power by doubling the photon amplification distance (Matuschek et al. 2017).

2 Models and parameters

Our analysis employs the commercial laser simulation software PICS3D by Crosslight Software Inc. which self-consistently combines carrier transport, quantum well (QW) band structure, spontaneous and stimulated photon emission, incl. ASE, wave guiding, as well as heat flow. Schrödinger and Poisson equations are solved iteratively in order to account for the QW energy band profile deformation with changing device bias due to the built-in polarization field. The transport model includes Fermi statistics, drift and diffusion of electrons and holes, as well as carrier loss mechanisms such as Shockley–Read–Hall (SRH) recombination, Auger recombination, and carrier leakage. More details on the laser model are published elsewhere (Piprek and Nakamura 2002; Piprek 2003).

The layer structure of our example device is shown in Table 1. It features two InGaN/GaN quantum wells sandwiched between GaN waveguide layers and AlGaN cladding layers. The electron blocking layer (EBL) was moved to the p-side edge of the waveguide in order to minimize the bias (Kawaguchi et al. 2016). The ridge waveguide is 12 µm wide and the cavity is 1.2 mm long. The measured light output power was $P = 7.2$ W at $I = 4$ A injection current in continuous-wave (CW) operation at room temperature (Kawaguchi et al. 2016). The high lasing power is based on an optimized ridge-waveguide structure with strongly reduced internal absorption ($\alpha_i = 2.5$ cm^{-1}) as well as on a low thermal resistance of about 7 K/W (Nozaki et al. 2016). However, due to the large series resistance, a

Table 1 Simulated layer structure (Kawaguchi et al. 2016)

Layer	Composition	Thickness (nm)	Refractive index
p-cladding	$Al_{0.026}Ga_{0.974}N$:Mg	660	2.520
p-EBL	$Al_{0.36}Ga_{0.64}N$:Mg	5	2.350
Waveguide	GaN	250	2.528
Waveguide	$In_{0.008}Ga_{0.992}N$	100	2.522
Quantum well	$In_{0.066}Ga_{0.934}N$	7.5	2.622
Barrier	$In_{0.008}Ga_{0.992}N$	20	2.522
Quantum well	$In_{0.066}Ga_{0.934}N$	7.5	2.622
Waveguide	$In_{0.008}Ga_{0.992}N$	40	2.522
Waveguide	GaN	450	2.528
n-cladding	$Al_{0.026}Ga_{0.974}N$:Si	900	2.520

high bias of V = 6.3 V was measured at 4 A which is about double the bias required by the photon energy (Piprek 2017b).

Key material parameters were obtained by simulating the measured laser performance (Piprek 2017a, see dashed lines in Fig. 1). The threshold current is mainly controlled by QW Auger recombination with a temperature-independent coefficient $C = 4.3 \times 10^{-30}$ cm^6/s, which lies within the range of reported numbers (Piprek et al. 2015). Defect-related SRH recombination has a negligible impact based on the SRH lifetime of 20 ns assumed inside the QWs. The slope efficiency is mainly limited by free-carrier absorption (Kawaguchi et al. 2016). We adopt a first-principle model for phonon-assisted free-carrier absorption (Kioupakis et al. 2010) which results in an absorption cross section of about 6×10^{-17} cm^2 in all layers (Piprek 2017a). Without further fitting, these parameters give good agreement with the measured laser power (Fig. 1). The measured bias V and input power IV are reproduced by calibrating the p-cladding hole mobility (2 cm^2/Vs) and the p-contact resistance ($R_c = 0.35\Omega$). The Mg acceptor density is 10^{20} cm^{-3} to reproduce the reported room-temperature free hole density of 10^{18} cm^{-3} in the p-cladding layer (Kawaguchi et al. 2016). Lateral uniform properties are assumed.

3 Results and discussion

Figure 1 compares LD and SLED characteristics calculated for CW operation at room temperature. The laser output power is more than double the SLED power which exhibits a power roll-off caused by self-heating. The bias hardly changes because layer structure and dimensions are the same for both devices. The slight bias difference is caused by the

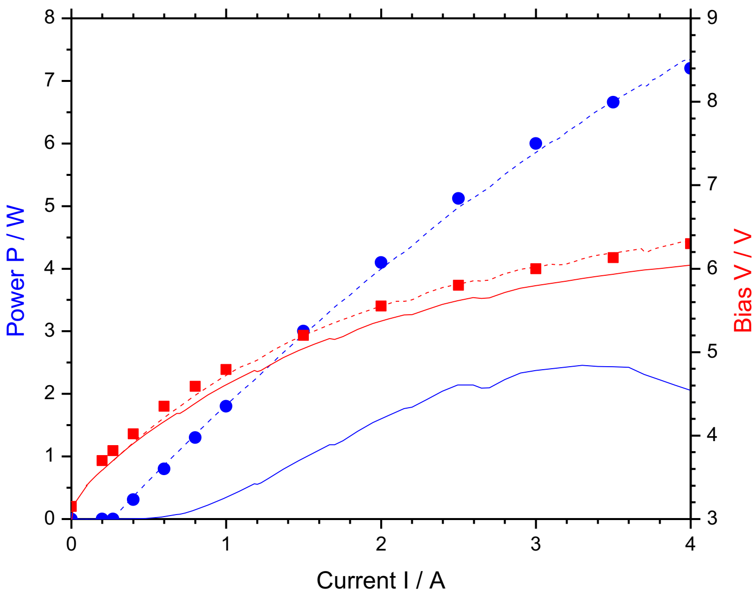

Fig. 1 Output power and bias simulated for the laser diode (dashed lines) and for the SLED (solid lines). Symbols show measured laser characteristics

self-heating which is somewhat stronger in the SLED ($\Delta T = 140$ K at 4 A) than in the laser (120 K), as expected from the lower SLED optical power.

Our SLED efficiency model is based on the approach commonly used for LEDs (Piprek 2016). While this approach is not typical for laser diodes (Piprek 2017a), it helps comparing the two device types here. The power conversion efficiency PCE = P/IV is defined as ratio of optical output power P to electrical input power IV (I—current, V—bias). The electrical efficiency ELE = hν/qV gives the ratio of emitted photon energy hν to injected electron energy qV. The internal quantum efficiency IQE is the fraction of the total electron current that is consumed by ASE or stimulated emission of photons. These key efficiencies are connected by PCE = ELE × IQE × EXE with the photon extraction efficiency EXE. The latter is hard to compare and not important here as it remains relatively high due to the low absorption and the low front facet reflectivity in both devices.

Figure 2 shows calculated results for the laser (dashed lines) and the SLED (solid lines). The total efficiency PCE peaks at 38% for the laser and at 15% for the SLED. It is severely limited by the electrical efficiency ELE which suffers from the low conductivity of p-doped waveguide layers (Piprek 2017a). The ELE droop with current imposes a similar efficiency reduction on both devices, since both employ the same waveguide structure. However, the strong PCE difference between SLED and laser is mainly caused by the IQE which suggests enhanced current losses in the SLED. Therefore, Fig. 3 compares all the internal processes that consume the injected current. Auger recombination represents by far the strongest current loss in both cases; it even surpasses the ASE current in the SLED. Spontaneous photon emission is also considered a loss because it goes in all directions, only a tiny fraction is coupled into the waveguide. Defect related SRH recombination is of minor importance here. However, these three current loss

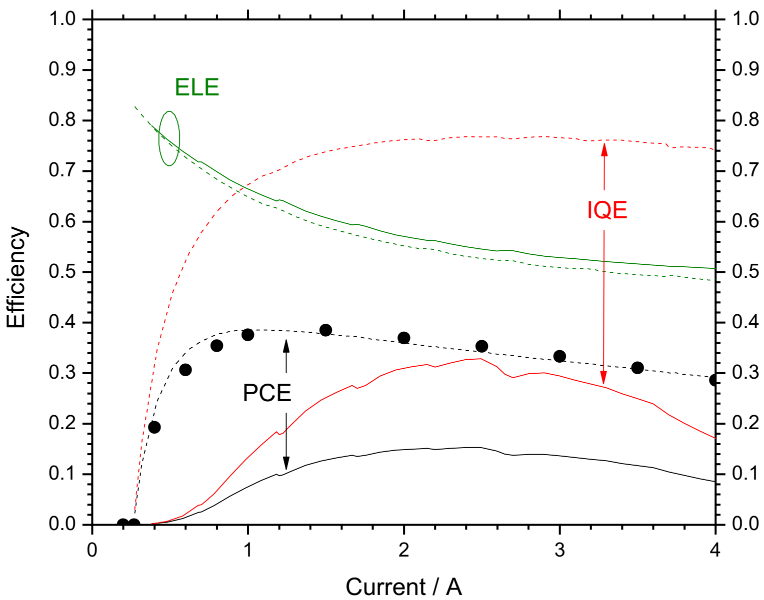

Fig. 2 Calculated efficiencies versus current for the laser diode (dashed lines) and for the SLED (solid lines). Symbols show the measured laser PCE

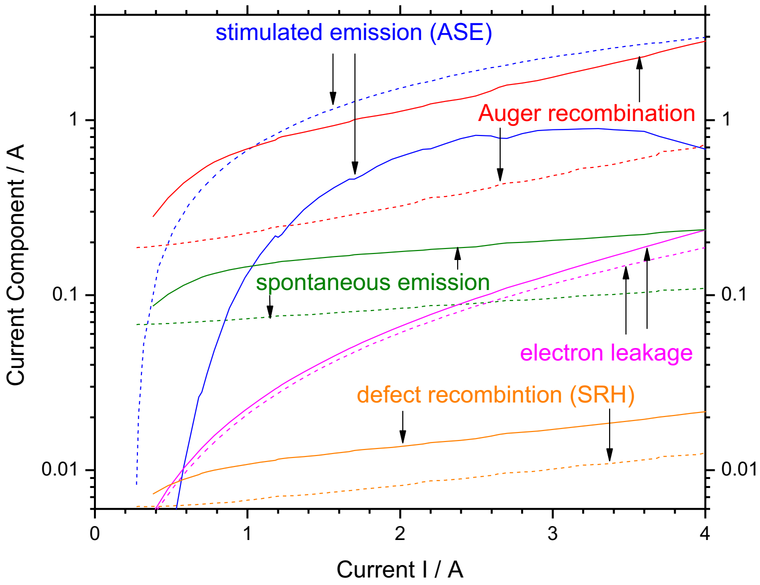

Fig. 3 Current components calculated for the laser (dashed lines) and for the SLED (solid lines)

mechanisms are much stronger in SLEDs than in lasers due to the higher QW carrier density. Electron leakage from the QWs is about the same for SLED and laser in Fig. 3.

Optical gain reduction with higher temperature causes a rising QW carrier density in both device types (Piprek 2017a). However, Fig. 4 reveals that this density is significantly larger in the SLED than in the laser because the former is operated below lasing threshold. Without self-heating, the QW carrier density of the laser remains constant above threshold while the SLED density keeps rising (Piprek 2020). This rising QW carrier density is therefore the key reason for the higher SLED carrier losses shown in Fig. 3.

In the following, we focus on the SLED and first study the impact of key parameters on the simulation results. Figure 5 shows that the removal of internal absorption from the model enhances the peak PCE only slightly to about 17% because the initial absorption was already low. Perfect heat sinking leads to PCE = 19% (no external thermal resistance, $\Delta T = 6$ K at 4 A) and removal of the contact resistance to PCE = 20%. Introduction of a small residual front facet reflectivity has a negligible effect on the efficiency but it leads to ripples in the ASE emission spectrum caused by longitudinal optical modes (Fig. 6). Practical SLEDs always exhibit a small residual front facet reflectivity which leads to lasing at higher current, so that the PCE peak in Fig. 2 is hard to reach experimentally.

Let's now look at design improvement options. QW recombination losses rise with the carrier density, which can be reduced by simply increasing the volume of the active layers. Resulting PCE characteristics are shown in Fig. 7. Increasing the chip length L is a common approach but it is limited by QW gain reductions at high photon densities (Matuschek et al. 2017). Tapered waveguide architectures reduce the photon density and the highest PCE achieved this way is 20% at our emission wavelength of 405 nm (Ohno et al. 2011). Another option is enlarging the total active layer thickness by using more or thicker QWs, which both results in higher SLED efficiencies.

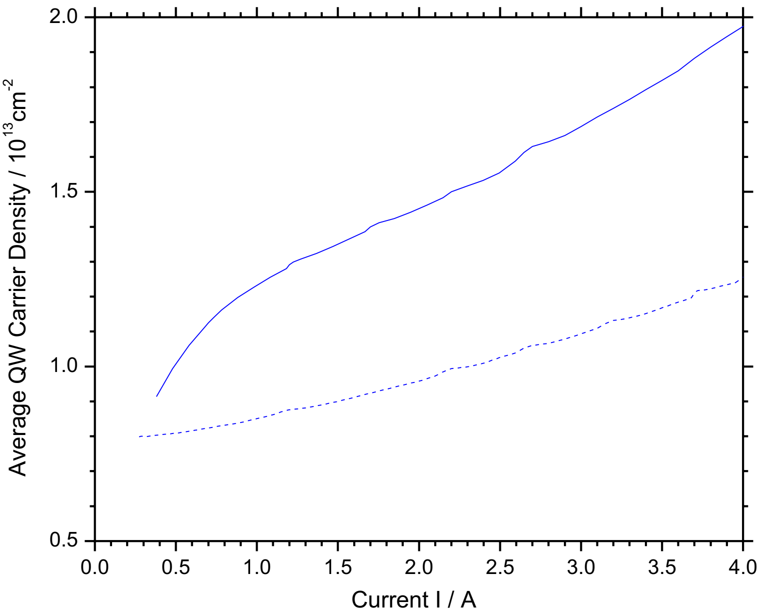

Fig. 4 Average carrier density inside the quantum wells for SLED (solid) and laser (dashed)

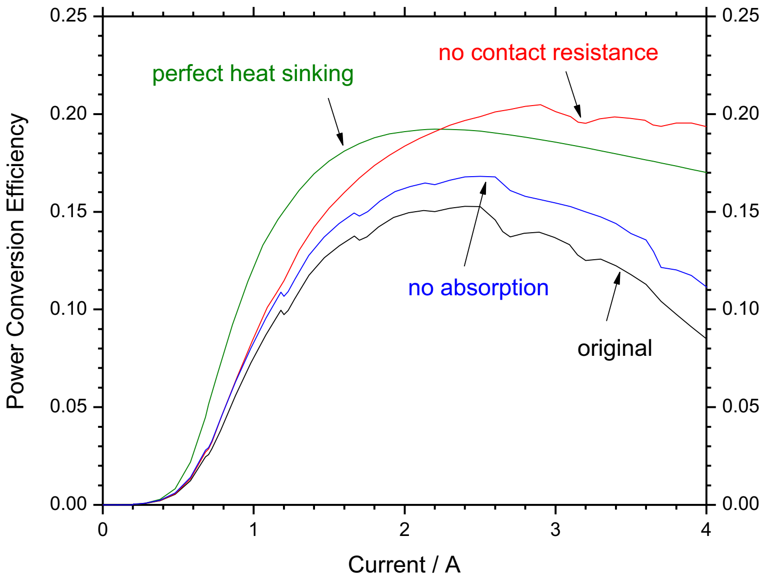

Fig. 5 Influence of key parameters on the simulated efficiency (PCE fluctuations are caused by numerical instabilities)

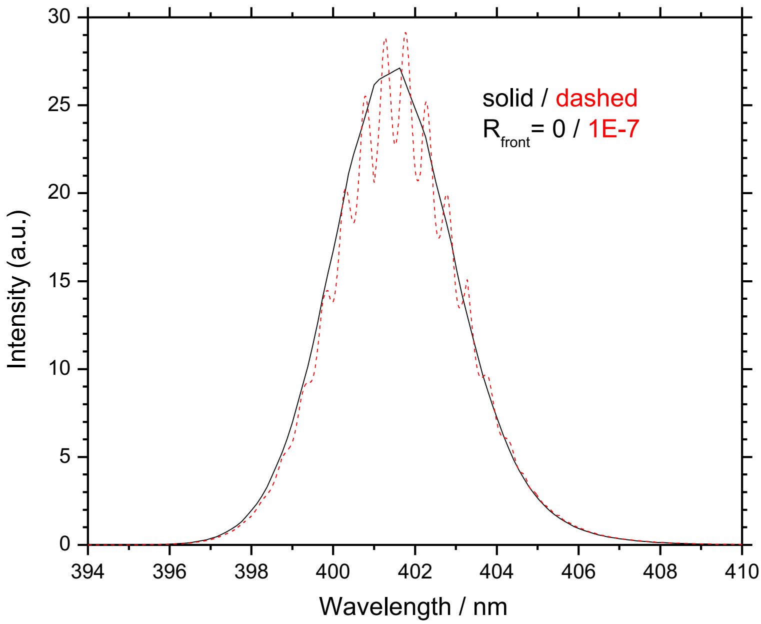

Fig. 6 SLED emission spectrum with different front facet reflectivity

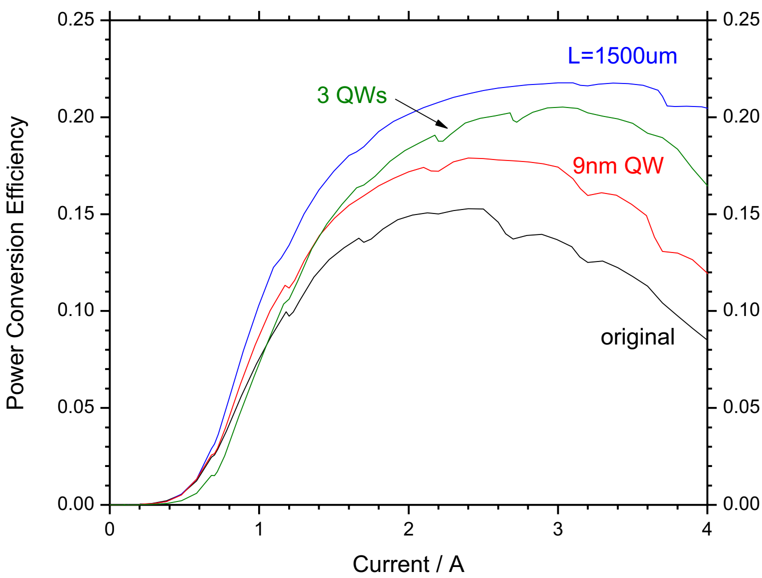

Fig. 7 Efficiency for different SLED design improvement options (PCE fluctuations are caused by numerical instabilities)

However, practical projection systems require somewhat longer wavelengths in the blue and green spectral region, that are generated by QWs with higher Indium content and lower band gap. This wavelength shift is accompanied by various challenges (Alatawi et al. 2018; Castiglia et al. 2018). QW growth quality and optical gain are severely reduced with longer wavelengths. The lower optical mode confinement leads to larger internal absorption, mainly in p-doped layers. Thus, above 440 nm emission wavelength, the highest reported PCE is still only 8% (Castiglia et al. 2018). Our efficiency analysis of blue light emitters is published elsewhere (Piprek 2020).

4 Summary

In conclusion, the power conversion efficiency of GaN-based SLEDs is severely limited by the low conductivity of p-doped waveguide layers, as in laser diodes. However, due to the higher quantum well carrier density, SLEDs suffer more than laser diodes from carrier recombination losses, in particular from Auger recombination, similar to LEDs. Efficiency enhancements can be achieved by enlarging the active volume of the SLED.

References

Alatawi, A.A., Holguin-Lerma, J.A., Kang, C.H., Shen, C., Subedi, R.S., Albardi, A.M., Alyamani, A.Y., Ng, T.K., Ooi, B.S.: High-power blue superluminescent diode for high CRI lighting and high-speed visible light communication. Opt. Express **26**, 26355–26364 (2018)

Castiglia, A., Rossetti, M., Malinverni, M., Mounir, C., Matuschek, N., et al.: Recent progress on GaN-based superluminescent light-emitting diodes in the visible range. SPIE Proc. **10532**, 1053421X (2018)

Hurni, C.A., David, A., Cich, M.J., Aldaz, R.I., et al.: Bulk GaN flip-chip violet light-emitting diodes with optimized efficiency for high-power operation. Appl. Phys. Lett. **106**, 031101 (2015)

Kawaguchi, M., Imafuji, O., Nozaki, S., Hagino, H., et al.: Optical-loss suppressed InGaN laser diodes using undoped thick waveguide structure. Proc. SPIE **9748**, 974818 (2016)

Kioupakis, E., Rinke, P., Van de Walle, C.: Determination of internal loss in nitride lasers from first principles. App. Phys. Express **3**, 082101 (2010)

Matuschek, N., Duelk, M.: In: Piprek, J. (ed.) Handbook of Optoelectronic Device Modeling and Simulation, vol. 19. CRC Press, Boca Raton (2017)

Nozaki, S., Yoshida, S., Yamanaka, K., Imafuji, O., et al.: High-power and high-temperature operation of an InGaN laser over 3 W at 85 °C using a novel double-heat-flow packaging technology. Jpn. J. Appl. Phys. **55**, 04EH05 (2016)

Ohno, H., Orita, K., Kawaguchi, M., Yamanaka, K., Takigawa, S.: 200 mW GaN-based superluminescent diode with a novel waveguide structure. In: IEEE Photonics Conference, WN2 (2011)

Piprek, J., Nakamura, S.: Physics of high-power InGaN/GaN lasers. IEE Proc. Optoelectr. **149**, 145151 (2002)

Piprek, J.: Semiconductor Optoelectronic Devices: Introduction to Physics and Simulation. Academic Press, San Diego (2003)

Piprek, J., Roemer, F., Witzigmann, B.: On the uncertainty of the Auger recombination coefficient extracted from InGaN/GaN light-emitting diode efficiency droop measurements. Appl. Phys. Lett. **106**, 101101 (2015)

Piprek, J.: Comparative efficiency analysis of GaN-based light-emitting diodes and laser diodes. Appl. Phys. Lett. **109**, 021104 (2016)

Piprek, J.: What limits the efficiency of high-power InGaN/GaN lasers? J. Quant. Electron. **53**, 2000104 (2017a)

Piprek, J.: What limits the power conversion efficiency of GaN-based lasers? Proc. SPIE **10098**, 100980Q (2017b)

Piprek, J.: Energy efficiency analysis of GaN-based blue light emitters. ECS J. Solid State Sci. Technol. **9**, 015008 (2020)

Rossetti, M., Napierala, J., Matuschek, N., Achatz, U., Duelk, M., Vélez, C., Castiglia, A., Grandjean, N., Dorsazc, J., Feltin, E.: Superluminescent light emitting diodes—the best out of two worlds. SPIE Proc. **8252**, 825208 (2012)

Strauss, U., Somers, A., Heine, U., Wurm, T., et al.: GaInN laser diodes from 440 to 530 nm: a performance study on single mode and multi-mode R&D designs. Proc. SPIE **10123**, 101230A (2017)

Publisher's Note Springer Nature remains neutral with regard to jurisdictional claims in published maps and institutional affiliations.